Communication Through Breath Using Molecular Communication Modeling in Indoor Environments

Thesis by

Nojood Almayouf

In Partial Fulfillment of the Requirements

For the Degree of

Master of Science

King Abdullah University of Science and Technology

Thuwal, Kingdom of Saudi Arabia

November, 2019

EXAMINATION COMMITTEE PAGE

The thesis of Nojood Almayouf is approved by the examination committee.

Committee Chairperson: Mohamed-Slim Alouini
Committee Co-Chair: Tareq Y. Al-Naffouri
Committee Members: Osama Amin, Hayssam Dahrouj

ABSTRACT

Communication Through Breath Using Molecular Communication Modeling in Indoor Environments

Nojood Almayouf

The concept of communication via breath is introduced under the molecular communication system, where data can be exchanged through inhalation and exhalation. Those data are carried by volatile organic compounds (VOCs) or pathogens and transferred through an aerosol channel. In this thesis, we propose a molecular communication model for an instantaneous source in a bounded indoor environment. The walls of this environment could be reflectors and/or absorbers by adjusting the value of deposition velocity. We assume a puff source in a given location and study the performance of a point source since it is the basic element that can be used to derive the concentration of breath, cough, and sneezing, where the concentration of continuous source can be found by integrating a point source over space and time domains. Also, we show some numerical results to visualize the performance of these mathematical models and evaluate them.

As a case study, we consider a real-life scenario of detecting a virus from an exhaled breath of a person standing in an indoor bounded room with reflective and absorptive walls. We derive the spatial-temporal concentration of an exhaled virus at the molecules source and the receiver in the room. Finally, we study the probability of misdetection using a suitable bio-sensor.

ACKNOWLEDGEMENTS

First, I want to thank God for enabling me to do this work. I would like to thank the committee members and my supervisors for their guidance and giving me the opportunity. Lastly but not least, I want to thank my family and friends for their love and support. Also, I would like to thank my colleagues and whoever helped me throughout the Master's journey.

TABLE OF CONTENTS

LIST OF FIGURES

Chapter 1

Communication Through Breath

In this chapter, we use a suitable bio-sensor thesis work by giving a background on molecular communication and the concept of communication through breath. First, we give some motivations followed by some existing work on the topic. Then, we highlight our contribution compared with existing related work. Finally, we describe the thesis outline and layout some notations.

1.1 Background and Objectives

Designing a reliable communication system between small-scale devices is a challenging and interesting engineering problem. Although radio communication systems are extensively used in our day-to-day activities such as several medical and industrial applications, it is not always feasible to deploy sensors and implement radio frequency communication systems. The size, cost and medium represent examples of the challenges that may restrict implementing traditional communication systems. For example, some objects of interest are located in minuscule regions that only can be reached by tiny materials. Moreover, developing a robust communication system that is capable of communicating in minute mediums has become a necessity, especially traditional communication systems mostly fail to fulfill the quality of service requirements. Molecular communication (MC) is introduced to address these issues by exchanging small-scale signals composed of molecules [1]. As a result, MC systems can be used in several applications related to biological engineering, healthcare, envi-

ronmental and industrial projects, where it can propose reliable, efficient small-scale communication solutions [2].

Recently, the concept of communication via breath is introduced under the umbrella of MC, where several data can be exchanged through inhalation and exhalation [3] [4]. The data are carried by VOCs or pathogens and transferred through an aerosol channel, where molecules spread by diffusion and advection. Exhaled VOCs represent bio-markers for the human body and give indications on body health such as infected diseases. These tiny particles are transferred in the atmospheric channel by diffusion and advection mechanisms, where the latter is controlled by (non)-artificial air flow [3].

Aerosol transmission is a very significant method for viral transmission in addition to other transmission methods that require physical contact. Influenza virus, which is an example of the viruses that can be spread via aerosol transmission [5] [6], has a serious negative impact on humanity and economy, e.g., in the U.S., influenza costs annually around $10.4 billion for hospitalization and outpatient visits for patients with age 18 years old and above [7]. Also, infectious viruses may develop into pandemics especially with the high number of international travels. Therefore, we can use the pathogenic aerosols in the exhaled breath to retrieve information that can be utilized to do appropriate actions.

In [8], Khalid *et al.* analyzed the steady-state concentration of pathogens in exhaled breath that spreads in the unbounded environment while applying artificial airflow. However, studying the instantaneous channel response in a bounded scenario is essential in analyzing the performance of several breath communication systems. To the best of the authors' knowledge, the existing research on MC does not study the channel response of MC channels in bounded environments with general absorption/reflection assumptions [9].

MC is used to analyze the exhaled/inhaled aerosol transmission, in which tiny

particles (VOCs or infectious pathogens) diffuse in the air and transfer by airflow. In light of analyzing the breath communication channel, [8] analyzed the pathogens concentration of exhaled breath in an unbounded environment. Moreover, in [9], a model for a rectangular duct channel with a point transmitter is presented, where the channels are bounded in x and y directions and unbounded in the z-direction with fully reflective walls.

In this thesis, we analyze the instantaneous spatial channel of MC in an indoor environment, where all propagation directions are bounded and subjected to full or partial absorption/reflection. To this end, we assume a point source in a given location and evaluate the received concentration of VOC/pathogens in the room while not applying controlled airflow. The spatial-temporal channel response can be used in analyzing both the exhaled or inhaled atmospheric breath channel. We study the performance of a puff source because it is the basic element that can be used to derive the concentration of breath, cough and sneezing by integrating the point source concentration performance over the underlying space and time dimensions.

1.2 Thesis Outline

This thesis is organized as follows. We start with some introduction and background about communication through breath. Then, we propose our system model in chapter 2. After that, we evaluate the concentration in total reflective, total reflective and partial absorptive, and partial absorptive environments in chapter $3, 4, 5$, respectively. In chapter 6, we propose a real-life scenario for detecting viruses from exhalation and we derive the probability of misdetection. Finally, we conclude with some results and potential future work.

1.3 Some Notation and Definitions

We denote the variable C in the x-dimension as C_x. Moreover, the partial derivative of C with respect to x is expressed as $\frac{\partial C}{\partial x}$ or $\frac{dC}{dx}$.

Chapter 2

Indoor System Model

In this chapter, we describe the indoor environment adopted in our model. Then, we explain the needed mathematical details to derive the main partial differential equation (PDE) for the VOCs concentration, whereas the solutions are proposed in the following three chapters.

2.1 Indoor Environment Description

We consider an MC system with a point source located in a bounded indoor environment and emits a VOC that propagates through the atmospheric channel as depicted in Fig. 2.1. The airflow helps in increasing the transmission range and decreasing the spreading delay. Such a scenario can be used to model the coughing or sneezing in a breath communication setup located in an indoor environment. We assume a bounded setup in the x, y, and z direction, where $0 < x < G_x$, $0 < y < G_y$, $0 < z < G_z$. Thus, the deposition velocity of the VOC at each room side determines the absorptivity level. For example, a zero deposition velocity represents a total reflector side, while a non-zero one reflects a partial absorption side.

In this work, we use the biosensor as a receiver to retrieve useful information about the transmitted VOC from a point source. Those pathogens reach the receiver side with the help of an artificial wind. The system is assumed to be bounded in an indoor environment. One possible application for such a system is a closed room that is established in locations with mass gatherings to test the people there whether they

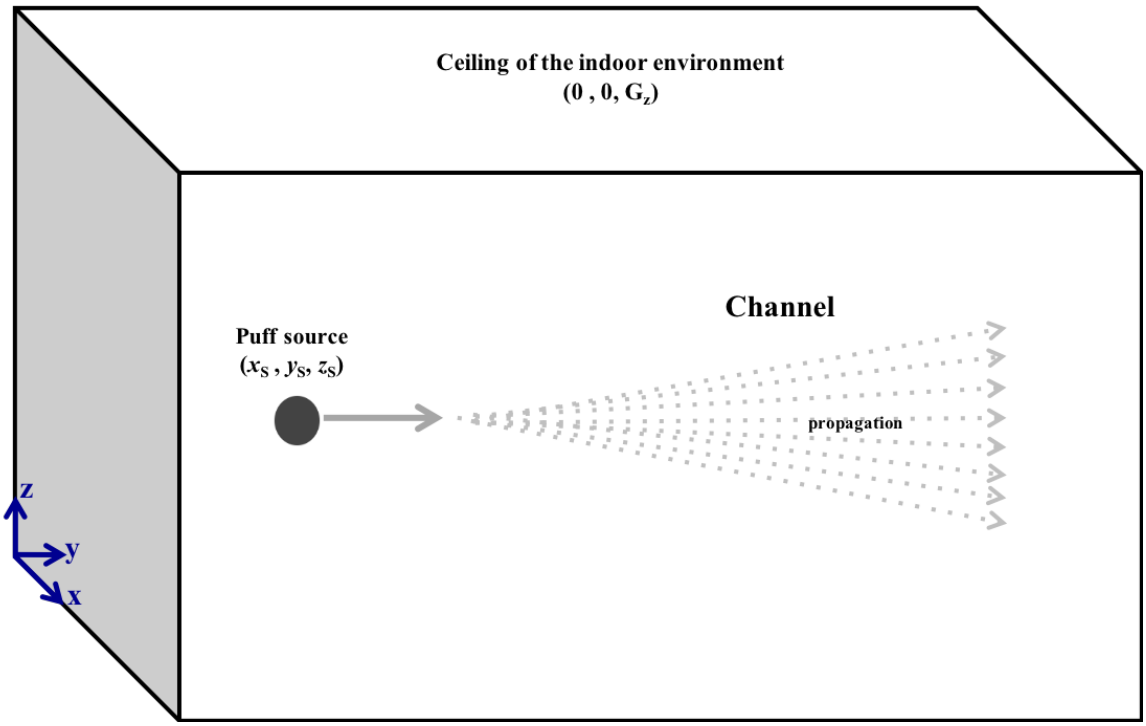

Figure 2.1: System setup for the proposed system.

are infected and non-infected.

2.2 Mathematical Modeling for Concentration

We model the indoor channel by evaluating the concentration, C (kg/m^3), of an emitted VOC/pathogen from an instantaneous point source that is located at (x_s, y_s, z_s) in a bounded room. The VOC particles are released and diffuse throughout the entire room without any airflow. To derive the mathematical model of C, we consider the mass conservation law, which states that the total mass of a system that has to be conserved within an elementary control volume $\Delta x \Delta y \Delta z$ (m^3), where Δx, Δy and Δz are the infinitesimal dimensions in x, y and z directions, respectively [10]. Thus, the total mass flux is controlled by particles diffusion according to [10]

$$\frac{\partial M}{\partial t} = D, \tag{2.1}$$

where M (kg) is the total mass where $M = C\Delta x\Delta y\Delta z$, $\frac{\partial M}{\partial t}$ is the mass flux (kg/s), i.e. the mass change with time, and D (kg/s) is the diffusion rate.

The particles turbulent diffusion represents the mass flux caused by eddies and is expressed for the same elementary volume as [10]

$$D = -\left[\frac{\partial F}{\partial x} + \frac{\partial F}{\partial y} + \frac{\partial F}{\partial z}\right]\Delta x\Delta y\Delta z, \tag{2.2}$$

where $\frac{\partial F}{\partial g},\ g \in \{x, y, z\}$ is the molecular diffusion change in the g direction and is expressed in terms of C according to Fick's law as $\frac{\partial F}{\partial g} = -K_g\frac{\partial C}{\partial g}$ [10], where $K_g(m^2/s)$ is the molecular diffusivity which is a constant that depends on the diffusive mass type and the surrounding fluid and the negative sign indicates that the flux direction is opposite to the concentration gradient. After plugging (2.2) in (2.1) and considering possible sources and chemical reactions that might change the concentration of particles, we get [10]

$$\frac{\partial C}{\partial t} = K_x\frac{\partial^2 C}{\partial x^2} + K_y\frac{\partial^2 C}{\partial y^2} + K_z\frac{\partial^2 C}{\partial z^2} + S + R, \tag{2.3}$$

where R $(kg/s \cdot m^3)$ is the concentration rate change due to any chemical reactions and S $(kg/s \cdot m^3)$ represents any sources and/or sinks that change the concentration rate. In this thesis, we assume that no chemical reaction could occur in the room. Thus, we can express C for different time intervals as

1. For $t < 0$, $C(x, y, z, t) = 0$.

2. For $t = t_{\mathrm{o}}$, $C(x, y, z, t) = Q\,\delta(x - x_{\mathrm{s}})\,\delta(y - y_{\mathrm{s}})\,\delta(z - z_{\mathrm{s}})$, where Q is the rate of emitted concentration starting at t_{o}.

3. For $t > t_{\mathrm{o}}$, C is found from the following PDE,

$$\frac{\partial C}{\partial t} = K_x\frac{\partial^2 C}{\partial x^2} + K_y\frac{\partial^2 C}{\partial y^2} + K_z\frac{\partial^2 C}{\partial z^2}. \tag{2.4}$$

To solve (2.4), we need to consider the following system initial condition (IC) and boundary conditions (BC's)

1. The initial VOC concentration is

$$C\left(x,y,z,t_{\mathrm{o}}\right)=Q\,\delta\left(x-x_{\mathrm{s}}\right)\delta\left(y-y_{\mathrm{s}}\right)\delta\left(z-z_{\mathrm{s}}\right)\delta\left(t-t_{\mathrm{o}}\right). \tag{2.5}$$

2. The room is bounded in the x, y, and z directions, where $0<x<G_x$, $0<y<G_y$, $0<z<G_z$.

3. Each room side exhibits different absorption and reflection characteristics, which is modeled mathematically as

$$K_g\frac{\partial C}{\partial g}=d_{g_i}C,\qquad g=g_i, \tag{2.6}$$

which is known as Robin boundary condition in PDE systems [11]. As mentioned previously $g\in\{x,y,z\}$ and $i=1,2,\ x_1=0,\ x_2=G_x,\ y_1=0,\ y_2=G_y,\ z_1=0,\ z_2=G_z$, and d_{g_i} is the deposition velocity in the g direction. d_{g_i} represents the level of absorptivity at a certain surface or wall, i.e., if the deposition velocity is equal to 0, then the surface is total reflector. while if d_{g_i} goes to infinity, the surface is a total absorber. In the following, we rewrite (2.6) as

$$\frac{\partial C}{\partial g}=\beta_{g_i},\quad g=\frac{d_{g_i}}{K_g}. \tag{2.7}$$

Now, using separation of variables, we write $C(x,y,z,t)$ as

$$C(x,y,z,t)=C_x\left(x,t\right)C_y\left(y,t\right)C_z\left(z,t\right). \tag{2.8}$$

To find C_x, C_y, and C_z. We follow the same approach in finding the concentration in the three directions x, y, z. Therefore, we show below the solution for the concen-

tration in the x direction, C_x and the same thing could be applied to find C_y and C_z.

Chapter 3

Evaluating Concentration in Total Reflective Environment

In this chapter, we evaluate the concentration of an emitted VOC/pathogen in an environment that has reflective walls, i.e., the deposition velocity is equal to zero and hence $\beta_{g_i} = 0$. We also discuss some simulation results at the end of the chapter.

3.1 Mathematical Derivation of the Concentration

The PDE that characterizes the concentration of the released particle is written as

$$\frac{\partial C}{\partial t} = K_x \frac{\partial^2 C}{\partial x^2} + K_y \frac{\partial^2 C}{\partial y^2} + K_z \frac{\partial^2 C}{\partial z^2}. \tag{3.1}$$

As mentioned previously, we will show the derivation of the concentration in the x-direction only, C_x, by solving the following ordinary differential equation (ODE). Then, C_y and C_z will have similar expressions. Thus, we consider now the following 1D PDE as

$$\frac{\partial C_x}{\partial t} = K_x \frac{\partial^2 C_x}{\partial x^2}, \tag{3.2}$$

with IC

$$C_x(x, t_{\mathrm{o}}) = \delta(x - x_{\mathrm{s}}), \tag{3.3}$$

and BC's

$$\frac{\partial C_x}{\partial x} = 0,\ x = 0, \tag{3.4}$$

$$\frac{\partial C_x}{\partial x} = 0,\ x = G_x. \tag{3.5}$$

The solution $C_x(x,t)$ can be expressed as a multiplication of the $X(x)$ and $T(t)$ components, i.e.,

$$C_x(x,t) = X(x)T(t). \tag{3.6}$$

We take the derivative of both sides with respect to t obtaining

$$\frac{\partial C_x}{\partial t} = X(x)\frac{\partial T(t)}{\partial t}, \tag{3.7}$$

From (3.7) and (3.2), we get

$$X(x)\frac{\partial T(t)}{\partial t} = K_x\frac{\partial^2 C_x}{\partial x^2}T(t). \tag{3.8}$$

Now, we divide both sides by $[K_x X(x)T(t)]$ obtaining

$$\frac{1}{X(x)}\frac{\partial^2 X(x)}{\partial x^2} = \frac{1}{K_{\mathrm{x}}T(t)}\frac{\partial T(t)}{\partial t} = -\lambda^2, \tag{3.9}$$

which can be written in another form as

$$\frac{dT(t)}{T(t)} = -\lambda^2 K_x dt. \tag{3.10}$$

We integrate both sides with respect to t getting

$$\ln|T(t)| = -\lambda^2 K_x t + H, \tag{3.11}$$

where H is a constant and hence we can have the $T(t)$ component as

$$T(t) = \mathrm{e}^{-K_x\lambda^2 t}H. \tag{3.12}$$

We find the $X(x)$ component from,

$$\frac{\partial^2 X(x)}{\partial x^2} + \lambda^2 X(x) = 0. \tag{3.13}$$

We consider two cases: the first one when $\lambda \neq 0$. We write (3.13) in a quadratic form as

$$r^2 + \lambda^2 = 0. \tag{3.14}$$

The above quadratic equation has two complex root $r_{1,2} = \pm i\lambda$. Also, it has a general solution on the form $X(x) = \mathrm{e}^{rx}$, Now, we plug those two roots to get,

$$X_1(x) = \mathrm{e}^{i\lambda x}, \tag{3.15}$$

$$X_2(x) = \mathrm{e}^{-i\lambda x}. \tag{3.16}$$

Using Euler's formula, (3.15) and (3.16) can be written as:

$$X_1(x) = \mathrm{e}^{i\lambda x} = \cos(\lambda x) + i\sin(\lambda x), \tag{3.17}$$

$$X_2(x) = \mathrm{e}^{-i\lambda x} = \cos(\lambda x) - i\sin(\lambda x), \tag{3.18}$$

We know in this case we can write the solution $X(x)$ as a linear combination of the two solutions,

$$X(x) = S_1\cos(\lambda x) + S_2\sin(\lambda x), \tag{3.19}$$

where S_1 and S_2 are constants. We take the first derivative of (3.19) with respect to x,

$$\frac{\partial X(x)}{\partial x} = -S_1\lambda\sin(\lambda x) + S_2\lambda\cos(\lambda x). \tag{3.20}$$

Using the first BC (3.4) and if $T(t) \neq 0$, we find that $S_2 = 0$. Moreover, from the second BC (3.5), we find

$$\sin(\lambda G_x) = 0, \tag{3.21}$$

where $\lambda = \frac{q\pi}{G_x}$ and q is an integer number. Therefore, the solution in this case is equal to

$$C_x(x,t) = \sum_{n=1}^{\infty} l_n X(x) T(t), \tag{3.22}$$

From what we found earlier using the BC's, we can write

$$C_x(x,t) = \sum_{n=1}^{\infty} l_n \cos(\lambda_n x) \mathrm{e}^{-K_x \lambda_n^2 t}, \tag{3.23}$$

and from the IC,

$$Q\delta(x - x_\mathrm{s}) = \sum_{n=1}^{\infty} l_n \mathrm{e}^{-K_x \lambda_n^2 t_\mathrm{o}} \cos(\lambda_n x) \tag{3.24}$$

Since $\{\cos(\lambda_n x)\}_{n=1}^{\infty}$ form basis of orthogonal functions, then using generalized Fourier series expansion, we can determine the generalized Fourier coefficients $[l_n \mathrm{e}^{-K_x \lambda_n^2 t}]$,

$$l_n \mathrm{e}^{-K_x \lambda_n^2 t_\mathrm{o}} = \frac{\langle \cos(\lambda_n x), Q\delta(x - x_\mathrm{s}) \rangle}{\langle \cos(\lambda_n x), \cos(\lambda_n x) \rangle}, \tag{3.25}$$

and

$$\langle \cos(\lambda_n x), Q\delta(x - x_\mathrm{s}) \rangle = \int_0^{G_x} \cos(\lambda_n x) Q\delta(x - x_\mathrm{s}) dx, \tag{3.26}$$

$$\langle \cos(\lambda_n x), \cos(\lambda_n x) \rangle = \int_0^{G_x} \cos^2(\lambda_n x) dx, \tag{3.27}$$

Hence, the generalized Fourier coefficient can be expressed as,

$$\frac{4Q\lambda_n \cos(\lambda_n x_\mathrm{s}) \mathrm{e}^{-K_x \lambda_n^2 (t - t_\mathrm{o})}}{2G_x \lambda_n + \sin(2G_x \lambda_n)}. \tag{3.28}$$

After substituting (3.28) in (3.23), the solution in this case can be expressed as

$$C_x(x,t) = \sum_{n=1}^{\infty} \frac{4Q\lambda_n \cos(\lambda_n x_s)\cos(\lambda_n x)e^{-K_x\lambda_n^2(t-t_o)}}{2G_x\lambda_n + \sin(2G\lambda_n)}. \tag{3.29}$$

From the identity, $[\sin(2G_x\lambda_n) = 2\sin(G_x\lambda_n)\cos(G_x\lambda_n)]$ and from the second BC, $\sin(G_x\lambda_n) = 0$, the solution is simplified into

$$C_x(x,t) = 2Q\sum_{n=1}^{\infty} \frac{\cos(\lambda_n x_s)\cos(\lambda_n x)e^{-K_x\lambda_n^2(t-t_o)}}{G_x}. \tag{3.30}$$

Now, for the second case when $\lambda = 0$, (3.13) becomes

$$\frac{\partial^2 X(x)}{\partial x^2} = 0, \tag{3.31}$$

Equation (3.31) has a general solution on the form $X(x) = W_1 + W_2 x$, where W_1 and W_2 are constants. The derivation of the solution with respect to x, $\frac{\partial X(x)}{\partial x}$, is equal to W_2. Now, we apply the BC's to know W_1 and W_2 as follows.

$$\frac{\partial X(0)}{\partial x} = 0 = W_2, \tag{3.32}$$

$$\frac{\partial X(G_x)}{\partial x} = 0 = W_2, \tag{3.33}$$

and hence W_2 is equal to zero and W_1 can be any value. Therefore, the complete solution of $C_x(x,t)$ can written as

$$C_x(x,t) = W_1 + 2Q\sum_{n=1}^{\infty} \frac{\cos(\lambda_n x_s)\cos(\lambda_n x)e^{-K_x\lambda_n^2(t-t_o)}}{G_x}, \tag{3.34}$$

where W_1 can be found using Fourier Cosine series. Using the IC, $C_x(x,t_o) = Q\delta(x - x_s)$, we have

$$Q\delta(x - x_s) = W_1 + 2Q\sum_{n=1}^{\infty} \frac{\cos(\lambda_n x_s)\cos(\lambda_n x)}{G_x} \tag{3.35}$$

and thus, W_1 could be found using Fourier Cosine series,

$$W_1 = \frac{1}{G_x} \int_0^{G_x} Q\delta(x - x_s)dx. \tag{3.36}$$

Thus, the concentration in the x- direction is expressed as

$$C_x(x,t) = \frac{Q}{G_x} + 2Q \sum_{n=1}^{\infty} \frac{\cos(\lambda_n x_{\mathrm{s}}) \cos(\lambda_n x) \mathrm{e}^{-K_x \lambda_n^2 (t - t_{\mathrm{o}})}}{G_x}. \tag{3.37}$$

3.2 Simulation Results

We simulate the concentration of a VOC in a bounded environment with fully reflective walls to visualize the concentration propagation over time and distance in the x, y, z direction.

We choose $x_s = 1m, x = 2.5m, G_x = 3m, Q = 10^{-3} kg/m^3 s, K_x = 1.64 \times 10^{-5} m^2/s$, and $t_{\mathrm{o}} = 0s$. The concentration at different times, i.e., from $t = 0s$ up to $t = 10 \times 10^5 s$ can be seen in Fig. 3.1. We can see that the concentration is starting from zero and increasing till it reaches a fixed value because the walls are reflective and hence, VOCs reserved inside the environment. This is not the case if one of the room's walls is an absorber.

For the same case, if we wanted to plot the concentration versus x with the same selected parameters but at different times $t = 20s, 100s, 500s, 1,000s, 50,000s, 100,000s$, and $200,000s$ as shown in Fig. 3.2 and 3.3. We see the concentration is maximized at $x = 1$ because the source of pathogen is located at $x_s = 1$. Also, if we increase the time to $200,000s$, we see the concentration is not changing (shown as a horizontal black line) because the walls of the room are reflective, and hence no molecules are absorbed in the room.

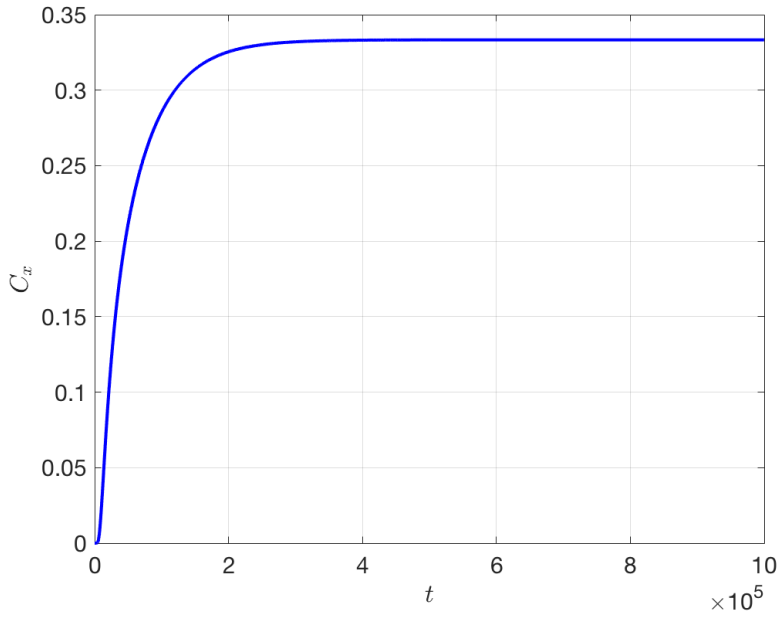

Figure 3.1: Concentration in the x-direction versus time for the case of total reflection.

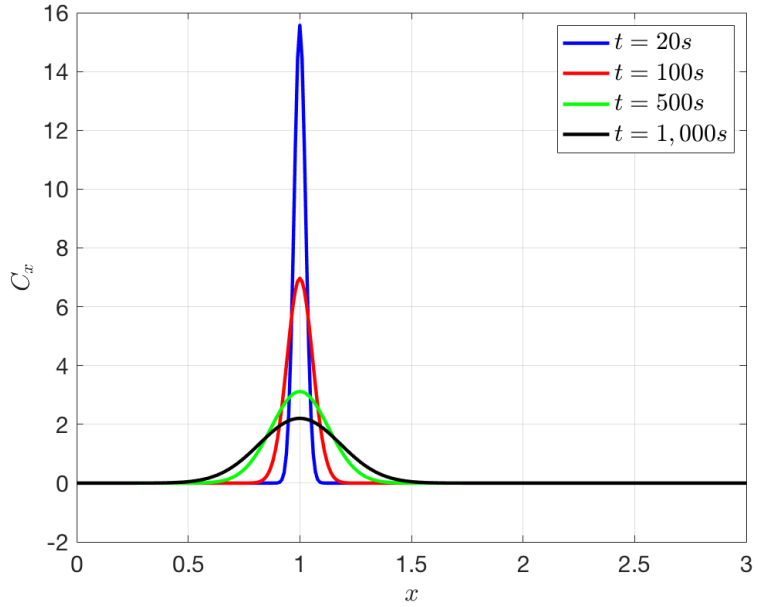

Figure 3.2: Concentration in the x-direction versus distance at different times for the case of total reflection.

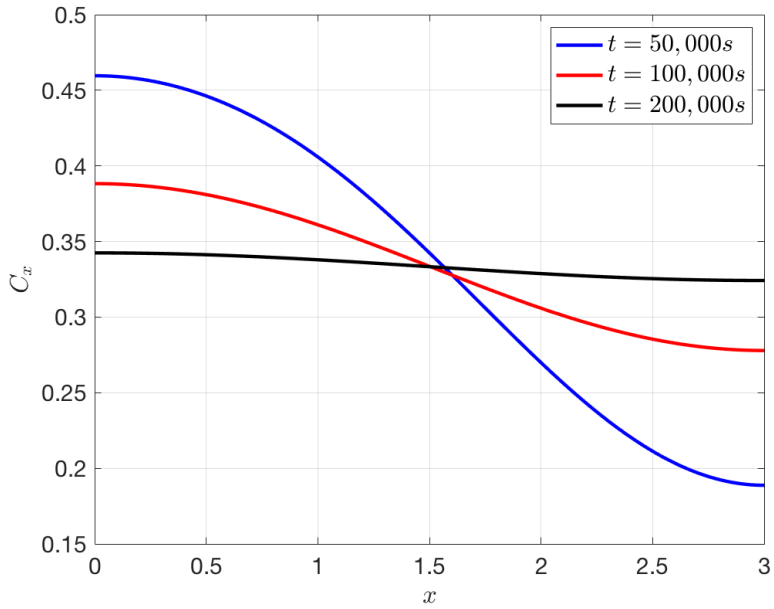

Figure 3.3: Concentration in the x-direction versus distance at different times for the case of total reflection.

Chapter 4

Evaluating Concentration in Partial Absorptive and Total Reflective Environment

In this chapter, we derive the concentration of a VOC/ pathogen in an environment that has reflective walls and partial absorptive, i.e., the deposition velocity of one of the walls is equal to zero. Moreover, for the other side, its deposition velocity has a value that is between zero and infinity. In addition to this, we discuss some simulation results to analyze the performance of the concentration.

4.1 Mathematical Derivation of the Concentration

We find C_x by solving the following ODE,

$$\frac{\partial C_x}{\partial t} = K_x \frac{\partial^2 C_x}{\partial x^2}, \tag{4.1}$$

with IC

$$C_x(x, t_{\mathrm{o}}) = Q\delta(x - x_{\mathrm{s}}), \tag{4.2}$$

and BC's

$$\frac{\partial C_x}{\partial x} = \beta_{x_1} C_x,\ x = 0, \tag{4.3}$$

$$\frac{\partial C_x}{\partial x} = 0,\ x = G_x, \tag{4.4}$$

We have our solution $C_x(x,t)$ as a multiplication of the $X(x)$ and $T(t)$ components, i.e.,

$$C_x(x,t) = X(x)T(t). \tag{4.5}$$

For the $T(t)$ component, we get the same solution as the one found in (3.12),

$$T(t) = \mathrm{e}^{-K_x\lambda^2 t}H. \tag{4.6}$$

Now, we find the $X(x)$ component from,

$$\frac{\partial^2 X(x)}{\partial x^2} + \lambda^2 X(x) = 0. \tag{4.7}$$

For $\lambda \neq 0$, we write the solution $X(x)$ in the same form as in chapter (3)

$$X(x) = S_1\cos(\lambda x) + S_2\sin(\lambda x). \tag{4.8}$$

We take the first derivative of (4.8) with respect to x obtaining

$$\frac{\partial X(x)}{\partial x} = -S_1\lambda\sin(\lambda x) + S_2\lambda\cos(\lambda x). \tag{4.9}$$

Using the first BC (4.3), we find that $S_2 = \frac{\beta_{x_1}S_1}{\lambda}$. Moreover, from the second BC (4.4) and if $T(t) \neq 0$, we find

$$\tan(\lambda G_x) = \frac{\beta_{x_1}}{\lambda}. \tag{4.10}$$

Therefor, the solution in this case is equal to

$$C_x(x,t) = \sum_{n=1}^{\infty} l_n X(x)T(t). \tag{4.11}$$

From what we found earlier using the BC's, we can write

$$C_x(x,t) = \sum_{n=1}^{\infty} l_n \big[S_1 \cos(\lambda_n x) + S_2 \sin(\lambda_n x)\big] \mathrm{e}^{-K_x \lambda_n^2 t}. \tag{4.12}$$

Substitute the value of S_2, we get

$$C_x(x,t) = \sum_{n=1}^{\infty} l_n \Big[S_1 \cos(\lambda_n x) + \frac{p_{x_1} S_1}{\lambda} \sin(\lambda_n x)\Big] \mathrm{e}^{-K_x \lambda_n^2 t}. \tag{4.13}$$

We let the weighting factor $(S_1 l_n) = l_n$

$$C_x(x,t) = \sum_{n=1}^{\infty} l_n \Big[\cos(\lambda_n x) + \frac{\beta_{x_1}}{\lambda} \sin(\lambda_n x)\Big] \mathrm{e}^{-K_x \lambda_n^2 t}, \tag{4.14}$$

and from (4.10), we can rewrite (4.14) as

$$\sum_{n=1}^{\infty} \frac{l_n \beta_{x_1}}{\lambda_n} \frac{1}{\sin(\lambda_n G)} \big[\cos(\lambda_n (G_x - x))\big] \mathrm{e}^{-K_x \lambda_n^2 t}, \tag{4.15}$$

From the IC, we write

$$Q\delta(x - x_{\mathrm{s}}) = \sum_{n=1}^{\infty} \frac{l_n \beta_{x_1}}{\lambda_n} \frac{\mathrm{e}^{-K_x \lambda_n^2 t_{\mathrm{o}}}}{\sin(\lambda_n G_x)} \big[\cos(\lambda_n (G - x))\big]. \tag{4.16}$$

Since $\{\cos(\lambda_n(G_x - x))\}_{n=1}^{\infty}$ form basis of orthogonal functions, then using generalized Fourier series expansion, we can determine the generalized Fourier coefficients $\left[\frac{l_n \beta_{x_1}}{\lambda_n} \frac{\mathrm{e}^{-K_x \lambda_n^2 t_{\mathrm{o}}}}{\sin(\lambda_n G_x)}\right]$ as,

$$\frac{l_n p_{x_1}}{\lambda_n} \frac{\mathrm{e}^{-K_x \lambda_n^2 t_{\mathrm{o}}}}{\sin(\lambda_n G_x)} = \frac{\langle \cos(\lambda_n (G - x)), Q\delta(x - x_{\mathrm{s}})\rangle}{\langle \cos(\lambda_n (G - x)), \cos(\lambda_n (G_x - x))\rangle}, \tag{4.17}$$

where

$$\langle \cos(\lambda_n (G_x - x)), Q\delta(x - x_{\mathrm{s}})\rangle = \int_0^{G_x} \cos(\lambda_n (G_x - x)) Q\delta(x - x_{\mathrm{s}}) dx, \tag{4.18}$$

$$\langle \cos(\lambda_n(G_x - x)), \cos(\lambda_n(G_x - x)) \rangle = \int_0^{G_x} \cos^2(\lambda_n(G_x - x))dx. \tag{4.19}$$

Hence, the generalized Fourier coefficient can be expressed as,

$$\frac{4Q\lambda_n \cos(\lambda_n(G_x - x_s))}{2G_x\lambda_n + \sin(2G_x\lambda_n)}. \tag{4.20}$$

After substituting (4.20) in (4.15), the solution in this case can be expressed as

$$C_x(x,t) = \sum_{n=1}^{\infty} \frac{4Q\lambda_n \cos(\lambda_n(G_x - x_s)) \cos(\lambda_n(G_x - x))}{2G_x\lambda_n + \sin(2G_x\lambda_n)} e^{-K_x\lambda_n^2(t-t_o)}, \tag{4.21}$$

From the identity, $[\sin(2G_x\lambda_n) = 2\sin(G_x\lambda_n)\cos(G_x\lambda_n)]$, the solution C_x is simplified into

$$C_x(x,t) = 2Q \sum_{n=1}^{\infty} \frac{(\lambda_n^2 + {\beta_{x_1}}^2) \cos(\lambda_n(G_x - x_s)) \cos(\lambda_n(G_x - x))}{G_x(\lambda_n^2 + {\beta_{x_1}}^2) + \beta_{x_1}} e^{-K_x\lambda_n^2(t-t_o)}. \tag{4.22}$$

4.2 Simulations Results

In this section, we show the concentration of a VOC/pathogen in a bounded environment that has one partially absorptive wall and one fully reflective wall to see the concentration propagation over time and distance in the x direction. In addition to the numerical values chosen in chapter (3), we set the deposition velocity d_{x_1} to $10,000m/s$. The concentration behavior versus time is shown in Fig. 4.1. We can see that the concentration is starting from zero and then it is increasing. Then, given one of the walls is an absorber, the concentration is decreasing when we increase the time till it reached almost zero.

We can also plot the concentration versus x with the same selected numerical values at different times $t = 20s, 100s, 500s,\ 1,000s, 50,000s, 100,000s$ and $200,000s$ as in Fig. 4.2 and 4.3. We can see that the maximum value of the concentration is at $x = 1$ because the initial point source is located at that location. Also, since the

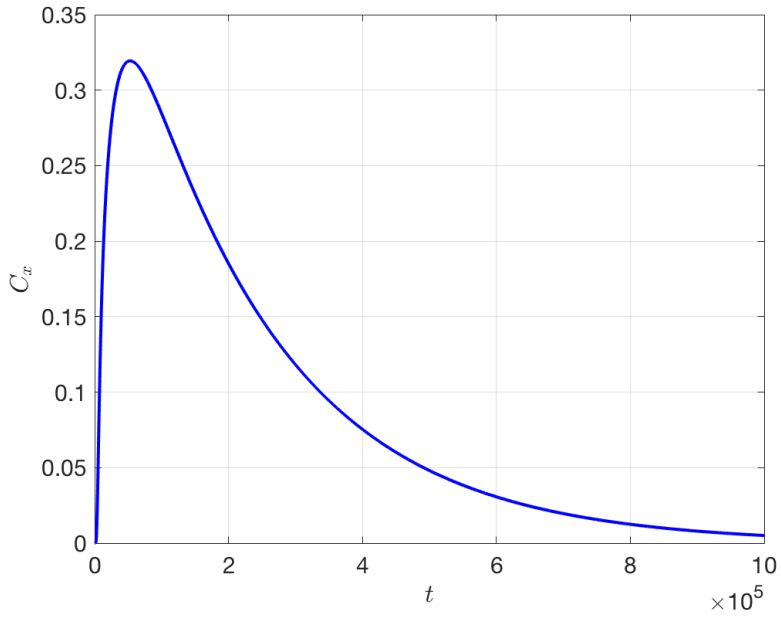

Figure 4.1: Concentration in the x-direction versus time for the case of total reflection and partial absorption.

wall at $x = 0$ is an absorber and the one at $x = 3$ is a reflector, it is clear in Fig. 4.3 that the concentration is high at $x = 3$ unlike at $x = o$.

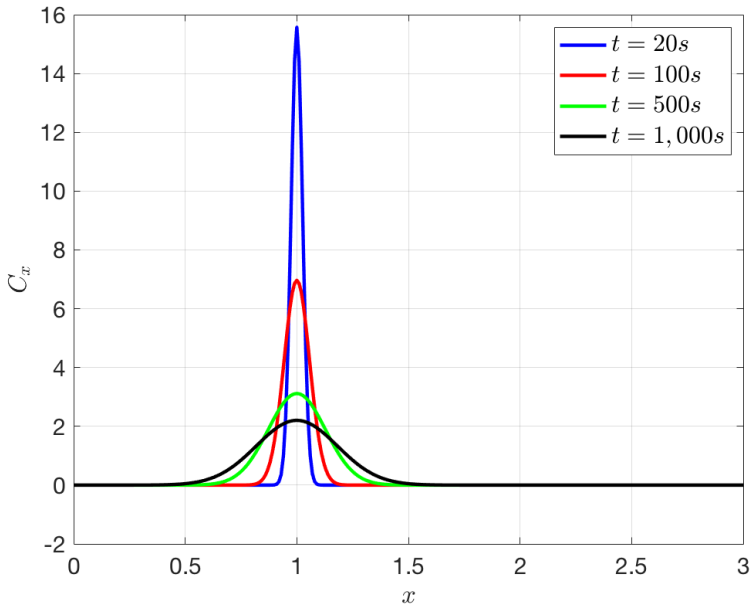

Figure 4.2: Concentration in the x-direction versus distance at different time for the case of total reflection and partial absorption.

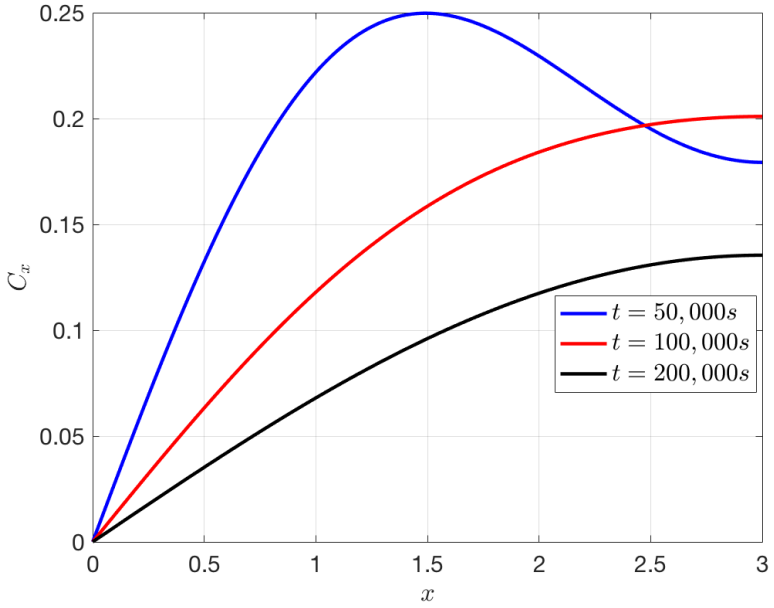

Figure 4.3: Concentration in the x-direction versus distance at different time for the case of total reflection and partial absorption.

Chapter 5

Evaluating Concentration in Partial Absorptive Environment

Here, we derive the concentration of molecules where the walls of the are partial absorptive. The absorptivity of the walls is controlled by the deposition velocity. The first wall where the molecules are emitted from has deposition velocity d_{x_1} and d_{x_2} where $\beta_{x_1} = \frac{d_{x_1}}{K_s}$ and $\beta = \frac{d_{x_2}}{K_x}$. In section 2 of this chapter, we show some simulation results for our mathematical model.

5.1 Mathematical Derivation of the Concentration

We find C_x by solving the following ODE,

$$\frac{\partial C_x}{\partial t} = K_x \frac{\partial^2 C_x}{\partial x^2}, \tag{5.1}$$

with IC

$$C_x(x, t_{\mathrm{o}}) = Q\delta(x - x_{\mathrm{s}}), \tag{5.2}$$

and BC's

$$\frac{\partial C_x}{\partial x} = \beta_{x_1} C_x,\ x = 0, \tag{5.3}$$

$$\frac{\partial C_x}{\partial x} = \beta_{x_2} C_x,\ x = G_x, \tag{5.4}$$

We have our solution $C_x(x,t)$ as a multiplication of the $X(x)$ and $T(t)$ components, i.e.,

$$C_x(x,t) = X(x)T(t). \tag{5.5}$$

For $T(t)$ component,the solution is the same as the one found in (3.12),

$$T(t) = \mathrm{e}^{-K_x\lambda^2 t}H. \tag{5.6}$$

Now, we find the $X(x)$ component from,

$$\frac{\partial^2 X(x)}{\partial x^2} + \lambda^2 X(x) = 0. \tag{5.7}$$

We consider two cases, when $\lambda \neq 0$ and $\lambda = 0$. For $\lambda \neq 0$, we write the solution $X(x)$ in the same form as in chapter (3)

$$X(x) = S_1\cos(\lambda x) + S_2\sin(\lambda x). \tag{5.8}$$

We take the first derivative of (5.8) with respect to x obtaining,

$$\frac{\partial X(x)}{\partial x} = -S_1\lambda\sin(\lambda x) + S_2\lambda\cos(\lambda x). \tag{5.9}$$

Using the first BC (5.3), we find that $S_2 = \frac{\beta_{x_1}S_1}{\lambda}$. Moreover, from the second BC (5.4), we find

$$\tan(\lambda G_x) = \frac{\lambda(\beta_{x_1} - \beta_{x_2})}{\beta_{x_1}\beta_{x_2} + \lambda^2}. \tag{5.10}$$

Therefore, the solution in this case is equal to

$$C_x(x,t) = \sum_{n=1}^{\infty} l_n X(x)T(t), \tag{5.11}$$

which is equivalent to

$$C_x(x,t) = \sum_{n=1}^{\infty} l_n \big[S_1 \cos(\lambda_n x) + S_2 \sin(\lambda_n x)\big] \mathrm{e}^{-K_x \lambda_n^2 t}. \tag{5.12}$$

From what was found using the first BC, we can substitute S_2 as follows

$$C_x(x,t) = \sum_{n=1}^{\infty} l_n \Big[S_1 \cos(\lambda_n x) + \frac{\beta_{x_1} S_1}{\lambda_n} \sin(\lambda_n x)\Big] \mathrm{e}^{-K_x \lambda_n^2 t}, \tag{5.13}$$

We let the weighting factor $(S_1 l_n) = l_n$

$$C_x(x,t) = \sum_{n=1}^{\infty} l_n \Big[\cos(\lambda_n x) + \frac{\beta_{x_1}}{\lambda_n} \sin(\lambda_n x)\Big] \mathrm{e}^{-K_x \lambda_n^2 t}. \tag{5.14}$$

To find l_n, we use the IC,

$$Q\delta(x - x_\mathrm{s}) = \sum_{n=1}^{\infty} l_n \mathrm{e}^{-K_x \lambda_n^2 t_\mathrm{o}} \Big[\cos(\lambda_n x) + \frac{\beta_{x_1}}{\lambda_n} \sin(\lambda_n x)\Big], \tag{5.15}$$

We find the generalized Fourier coefficients $l_n \mathrm{e}^{-K_x \lambda_n^2 t_\mathrm{o}}$ from the generalized Fourier series expansion because $\Big\{ \Big[\cos(\lambda_n x) + \frac{\beta_{x_1}}{\lambda_n} \sin(\lambda_n x)\Big] \Big\}_{n=1}^{\infty}$ form basis of orthogonal functions as it is proven in appendix A, hence we have

$$l_n \mathrm{e}^{-K_x \lambda_n^2 t_\mathrm{o}} = \frac{\Big\langle \cos(\lambda_n x) + \frac{\beta_{x_1}}{\lambda_n} \sin(\lambda_n x), Q\delta(x - x_\mathrm{s}) \Big\rangle}{\Big\langle \cos(\lambda_n x) + \frac{\beta_{x_1}}{\lambda_n} \sin(\lambda_n x), \cos(\lambda_n x) + \frac{\beta_{x_1}}{\lambda_n} \sin(\lambda_n x) \Big\rangle}, \tag{5.16}$$

where

$$\begin{aligned} &\Big\langle \cos(\lambda_n x) + \frac{\beta_{x_1}}{\lambda_n} \sin(\lambda_n x), Q\delta(x - x_\mathrm{s}) \Big\rangle \\ &= \int_0^{G_x} \cos(\lambda_n x) + \frac{\beta_{x_1}}{\lambda_n} \sin(\lambda_n x) Q\delta(x - x_\mathrm{s}) dx, \end{aligned} \tag{5.17}$$

$$\Big\langle \cos(\lambda_n x) + \frac{\beta_{x_1}}{\lambda_n} \sin(\lambda_n x), \cos(\lambda_n x) + \frac{\beta_{x_1}}{\lambda_n} \sin(\lambda_n x) \Big\rangle$$

$$= \int_0^{G_x} \Big(\cos(\lambda_n x) + \frac{\beta_{x_1}}{\lambda_n} \sin(\lambda_n x) \Big)^2 dx. \tag{5.18}$$

The generalized Fourier coefficient can be expressed as,

$$\frac{4Q\lambda_n^3 \Big(\cos(\lambda_n x_s) + \frac{\beta_{x_1}}{\lambda} \sin(\lambda_n x_s) \Big)}{(\lambda_n^2 - \beta_{x_1}^2)\sin(2\lambda_n G) - 4\beta_{x_1}\lambda_n \cos^2(\lambda_n G) + 2G\lambda_n^3 + \lambda_n(2\beta_{x_1}^2 G + 4\beta_{x_1})}. \tag{5.19}$$

After substituting (5.19) in (5.14), the solution in this case can be expressed as

$$C_x(x,t) = 4Q \sum_{n=1}^{\infty} \frac{\lambda_n^3 \Big(\cos(\lambda_n x_s) + \frac{\beta_{x_1}}{\lambda_n} \sin(\lambda_n x_s) \Big) \Big(\cos(\lambda_n x) + \frac{\beta_{x_1}}{\lambda_n} \sin(\lambda_n x) \Big) \mathrm{e}^{-K_x \lambda_n^2 (t - t_\mathrm{o})}}{(\lambda_n^2 - \beta_{x_1}^2)\sin(2\lambda_n G) - 4\beta_{x_1}\lambda_n \cos^2(\lambda_n G) + 2G\lambda_n^3 + \lambda_n(2\beta_{x_1}^2 G + 4\beta_{x_1})}, \tag{5.20}$$

For the second case when $\lambda = 0$, we write (5.7) as

$$\frac{\partial^2 X(x)}{\partial x^2} = 0, \tag{5.21}$$

which has a general solution $X(x) = W_1 + W_2 x$, where W_1 and W_2 are constants. To find these two constants, we apply the BC's as follows,

$$\frac{\partial X(0)}{\partial x} = \beta_{x_1} X(0) = W_2, \tag{5.22}$$

$$\frac{\partial X(G_x)}{\partial x} = \beta_{x_2} X(G) = W_2. \tag{5.23}$$

Hence, we can write $W_2 = \frac{w_1(\beta_{x_1} - \beta_{x_2})}{\beta_{x_2} G_x}$ and the complete solution of $C_x(x,t)$ can be expressed as

$$C_x(x,t) = W_1 + \frac{w_1(\beta_{x_1} - \beta_{x_2})}{\beta_{x_2} G_x} x +$$

$$4Q \sum_{n=1}^{\infty} \frac{\lambda_n^3 \Big(\cos(\lambda_n x_s) + \frac{\beta_{x_1}}{\lambda_n} \sin(\lambda_n x_s) \Big) \Big(\cos(\lambda_n x) + \frac{\beta_{x_1}}{\lambda_n} \sin(\lambda_n x) \Big) \mathrm{e}^{-K_x \lambda_n^2 (t - t_\mathrm{o})}}{(\lambda_n^2 - \beta_{x_1}^2)\sin(2\lambda_n G) - 4\beta_{x_1}\lambda_n \cos^2(\lambda_n G) + 2G\lambda_n^3 + \lambda_n(2\beta_{x_1}^2 G + 4\beta_{x_1})}, \tag{5.24}$$

We can find W_1 using Fourier Series. Using the IC, $C_x(x,t_o) = Q\delta(x-x_s)$, we get

$$Q\delta(x-x_s) - \frac{w_1(\beta_{x_1}-\beta_{x_2})}{\beta_{x_2}G_x}x = W_1 +$$

$$4Q\sum_{n=1}^{\infty}\frac{\lambda_n^3\Big(\cos(\lambda_n x_s)+\frac{\beta_{x_1}}{\lambda_n}\sin(\lambda_n x_s)\Big)\Big(\cos(\lambda_n x)+\frac{\beta_{x_1}}{\lambda_n}\sin(\lambda_n x)\Big)}{(\lambda_n^2-\beta_{x_1}^2)\sin(2\lambda_n G)-4\beta_{x_1}\lambda_n\cos^2(\lambda_n G)+2G\lambda_n^3+\lambda_n(2\beta_{x_1}^2G+4\beta_{x_1})} \tag{5.25}$$

where W_1 could be found as,

$$W_1 = \frac{1}{G_x}\int_0^{G_x} Q\delta(x-x_s)dx - \frac{w_1(\beta_{x_1}-\beta_{x_2})}{\beta_{x_2}G_x}\int_0^{G_x} x dx, \tag{5.26}$$

Thus, the concentration in the x- direction is expressed as

$$C_x(x,t) = \frac{2Q\beta_{x_2}}{2\beta_{x_2}G+G(\beta_{x_1}-\beta_{x_2})} + \frac{2Q(\beta_{x_1}-\beta_{x_2})}{G^2(\beta_{x_2}+\beta_{x_1})}x +$$

$$+ 4Q\sum_{n=1}^{\infty}\frac{\lambda_n^3\Big(\cos(\lambda_n x_s)+\frac{\beta_{x_1}}{\lambda_n}\sin(\lambda_n x_s)\Big)\Big(\cos(\lambda_n x)+\frac{\beta_{x_1}}{\lambda_n}\sin(\lambda_n x)\Big)\mathrm{e}^{-K_x\lambda_n^2(t-t_o)}}{(\lambda_n^2-\beta_{x_1}^2)\sin(2\lambda_n G)-4\beta_{x_1}\lambda_n\cos^2(\lambda_n G)+2G\lambda_n^3+\lambda_n(2\beta_{x_1}^2G+4\beta_{x_1})}. \tag{5.27}$$

5.2 Simulations Results

In this section, we show the concentration of VOCs in a bounded environment that has partially absorptive walls.

We plot the concentration of pathogens versus the distance. In addition to the parameters' values we choose in the previous sections, we choose the deposition velocity of the first wall to be $100,000 m/s$ while the deposition velocity of the second wall at $x = 3$ to be $10^{-5} m/s$. In Fig. 5.1, we see that the concentration has the highest value at $x = 1$ as it is the initial point location for the emitted molecules. Moreover, since the deposition velocity of the wall at $x = 3$ is very low, i.e., which makes it almost a reflector, the concentration is higher when we are close to $x = 3$ than when we are at

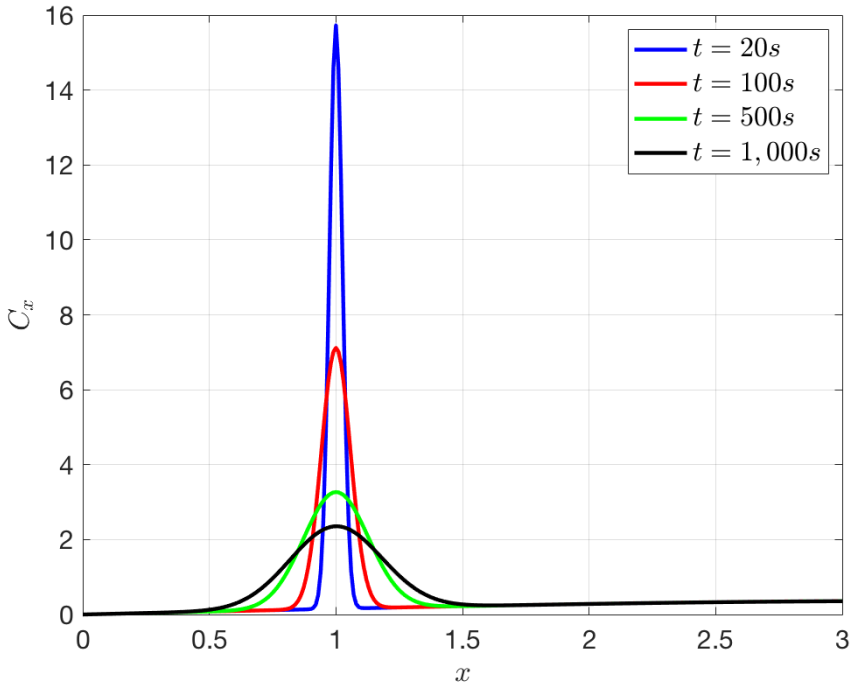

Figure 5.1: Concentration in the x-direction versus distance at different time for the case of partial absorption.

$x = 0$. This can be seen very clearly in Fig. 5.2 with a high t value.

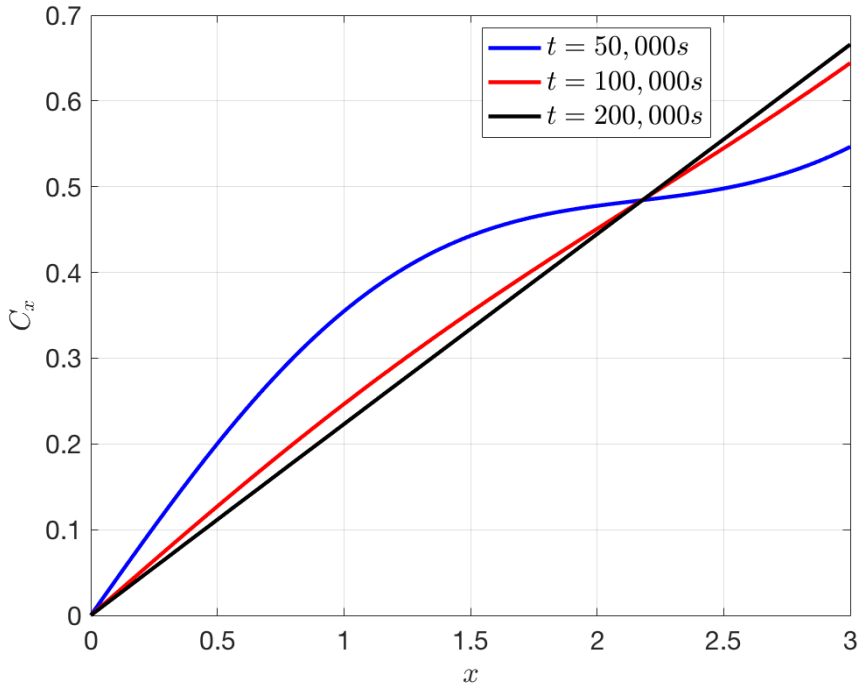

Figure 5.2: Concentration in the x-direction versus distance at different time for the case of partial absorption.

Chapter 6

Virus Detection from Exhaled Breath in Indoor Environment

In this chapter, we consider a real-life scenario for detecting viruses from exhaled breath. We propose the system model and the steps done to derive the probability of misdetection. Finally, we present a graph for the probability of misdetection to show the performance of the system model for different distance and emission rate of Q.

6.1 Scenario Description

A real-life example for detecting viruses from exhaled breath is shown in Fig. (6.1) where a person is standing at (x_s, y_s, z_s) in an indoor bounded room with partial absorption and total reflection sides. We assume an exhalation breath scenario, where the exhaled breath is released with a velocity less than $140 cm/s$ [12]. The exhaled breath speed decreases forming a maximum drifting distance [12]. We model the released exhaled cloud as a cuboid shown in Fig. 6.1 to simplify the analysis. The outer faces of the cuboid represent planar sources of released particles that have approximately zero velocity [12].

In the rest of this chapter, we study the concentration of a virus that is released from the five outer planar sources and diffuse in a room as shown in Fig. 6.1. For the receiver, it is shown as a blue cube and the coordinates of each side are written on the figure.

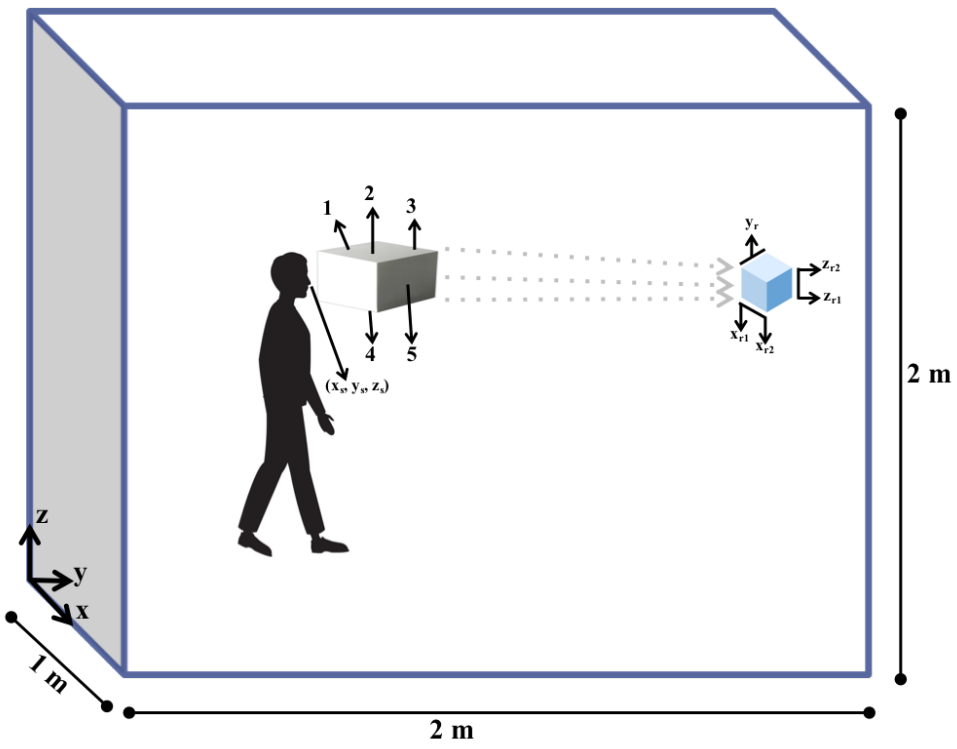

Figure 6.1: Proposed system for detecting viruses from exhalation

6.2 Concentration at the Receiver

Now, we want to measure the concentration at the receiver. To do so, we need to know the concentration of pathogens inside the receiving cube. We start from the expression of the concentration for a partial absorptive and total reflective environment without airflow for a puff source. From (4.22) in chapter (4), the expression is written as,

$$C_x(x,t) = 2Q \sum_{n=1}^{\infty} \frac{(\lambda_n^2 + \beta_{x1}^2)\cos(\lambda_n(G_x - x_s))\cos(\lambda_n(G_x - x))}{G_x(\lambda_n^2 + \beta_{x1}^2) + \beta_{x1}} e^{-K_x\lambda_n^2(t-t_s)} \tag{6.1}$$

To find the concentration of a planar source, we need to consider point sources arranged in a planar form and find the total concentration by taking the integration over different point source locations. That concentration should be found considering the three dimensions $x, y,$ and z, i.e., $C_i(x,y,z,t) = C_x, C_y,$ and C_z, where $i =$

$1, 2, 3, 4, 5..$ Hence, the concentration of the pathogens on the cuboid sides can be found from the following expression where each side is a $2D$ plane and has different boundary limits based on the location of that planar.

$$C_s(x,y,z,t) = \int_{y_s}\int_{z_s}\int_{t_s} C_1(x,y,z,t)dt_s dz_s dy_s + \int_{y_s}\int_{x_s}\int_{t_s} C_2(x,y,z,t)dt_s dx_s dy_s + \int_{x_s}\int_{z_s}\int_{t_s} C_3(x,y,z,t)dt_s dz_s dx_s + \int_{x_s}\int_{y_s}\int_{t_s} C_4(x,y,z,t)dt_s dy_s dx_s + \int_{z_s}\int_{y_s}\int_{t_s} C_5(x,y,z,t)dt_s dy_s dz_s \quad (6.2)$$

In the following, we evaluate the first term and then a similar approach can be followed to evaluate other integrations.

$$\int_{z_s}\int_{y_s}\int_{t_s} C_1(x,y,z,t)dt_s dy_s dz_s = \int_{y_s}\int_{z_s}\int_{t_s} (2)^3 Q \sum_{n=1}^{\infty} \left[\frac{(\lambda_n^2+\beta_{x1}^2)\cos(\lambda_n(G_x-x_s))\cos(\lambda_n(G_x-x))}{G_x(\lambda_n^2+\beta_{x1}^2)+\beta_{x1}} \frac{(\lambda_n^2+\beta_{y1}^2)\cos(\lambda_n(G_y-y_s))\cos(\lambda_n(G_y-y))}{G_y(\lambda_n^2+\beta_{y1}^2)+\beta_{y1}} \frac{(\lambda_n^2+\beta_{z1}^2)\cos(\lambda_n(G_z-z_s))\cos(\lambda_n(G_z-z))}{G_z(\lambda_n^2+\beta_{z1}^2)+\beta_{z1}} e^{-\lambda_n^2(t-t_s)(K_x+K_y+K_z)} e^{-k_x\lambda_n^2(t-t_s)} \right] dt_s dy_s dz_s \quad (6.3)$$

After computing the concentration, we get

$$\int_{z_s}\int_{y_s}\int_{t_s} C_1(x,y,z,t)dt_s dy_s dz_s = \sum_{n=1}^{\infty}(2)^3 Q \frac{e^{-\lambda_n^2 t(K_x+K_y+K_z)}\left(e^{\lambda_n^2 t(K_x+K_y+K_z)} - e^{-\lambda_n^2 t_0(K_x+K_y+K_z)}\right)}{\lambda_n^2(K_x+K_y+K_z)} \frac{(\lambda_n^2+\beta_{x1}^2)\cos(\lambda_n(G_x-x_s))\cos(\lambda_n(G_x-x))}{G_x(\lambda_n^2+\beta_{x1}^2)+\beta_{x1}} \frac{(\lambda_n^2+\beta_{y1}^2)\cos(\lambda_n(G_y-y))}{G_y(\lambda_n^2+\beta_{y1}^2)+\beta_{y1}}\left(-\frac{\sin(\lambda_n(G_y-y_{s_2}))}{\lambda_n}+\frac{\sin(\lambda_n(G_y-y_{s_1}))}{\lambda_n}\right) \frac{(\lambda_n^2+\beta_{z1}^2)\cos(\lambda_n(G_z-z))}{G_z(\lambda_n^2+\beta_{z1}^2)+\beta_{z1}}\left(-\frac{\sin(\lambda_n(G_z-z_{s_1}))}{\lambda_n}+\frac{\sin(\lambda_n(G_z-z_{s_1}))}{\lambda_n}\right) \tag{6.4}$$

Now, the second step to find the probability of misdetection is to find the average concentration of viruses at the receiver side, C_{mean},

$$C_{\text{mean}} = \int_{z_{r_1}}^{z_{r_2}}\int_{y_r-\Delta y}^{y_r+\Delta y}\int_{x_{r_1}}^{x_{r_2}}\int_{t_0}^{t_0+T_s} C_s(x,y,z,t)dtdxdydz \tag{6.5}$$

where $C_s(x,y,z,t)$ is the resulting integration for the five sides of the grey cube, $x_{r_1}, x_{r_2}, y_{r_q}, y_{r_2}, z_{r_1}, z_{r_2}$ are the coordinates of the receiver along x, y, and z direction, respectively. Moreover, Δy indicates how much the receiver is moving along the y-direction and T_s is the sampling time.

To evaluate the virus concentration at the receiving side, we find the captures virus inside the receiver volume and after T_s. The concentration mean is computed as a superposition of the received viruses due to the five planar surfaces. In the following, we show the concentration mean due to one surface, and the contribution

of other surfaces can be found using similar computations.

$$C_{\text{mean}_1} = \frac{2^3 Q}{\lambda_n^2(K_x+K_y+K_z)}\Bigg[\frac{e^{\lambda_n^2 t_0(K_x+K_y+K_z)-\lambda_n^2 t_0(K_x+K_y+K_z)(t_0+T_s)}}{\lambda_n^2(K_x+K_y+K_z)} + (t_0+T_s) - \frac{1}{\lambda_n^2(K_x+K_y+K_z)} - t_0\Bigg]$$
$$\frac{(\lambda_n^2+\beta_{x1}^2)\cos(\lambda_n(G_x-x_s))}{G_x(\lambda_n^2+\beta_{x1}^2)+\beta_{x1}}\left(-\frac{\sin(\lambda_n(G_x-x_{r_2}))}{\lambda_n}+\frac{\sin(\lambda_n(G_x-x_{r_1}))}{\lambda_n}\right)$$
$$\frac{(\lambda_n^2+\beta_{y1}^2)}{G_y(\lambda_n^2+\beta_{y1}^2)+\beta_{y1}}\left(-\frac{\sin(\lambda_n(G_y-y_{s_2}))}{\lambda_n}+\frac{\sin(\lambda_n(G_y-y_{s_1}))}{\lambda_n}\right)$$
$$\left(-\frac{\sin(\lambda_n(G_y-(y_{r_2}+0.2)))}{\lambda_n}+\frac{\sin(\lambda_n(G_y-(y_{r_1}-0.2)))}{\lambda_n}\right)$$
$$\frac{(\lambda_n^2+\beta_{z1}^2)}{G_z(\lambda_n^2+\beta_{z1}^2)+\beta_{z1}}\left(-\frac{\sin(\lambda_n(G_z-z_{s_2}))}{\lambda_n}+\frac{\sin(\lambda_n(G_z-z_{s_1}))}{\lambda_n}\right)$$
$$\left(-\frac{\sin(\lambda_n(G_z-z_{r_2}))}{\lambda_n}+\frac{\sin(\lambda_n(G_z-z_{r_1}))}{\lambda_n}\right) \quad (6.6)$$

In general, a molecular receiver is affected by, at least, four types of noises [3]: binding noise, flicker noise, thermal noise, and interference noise between different types of viruses. However, we assume the indoor environment to be sanitized before doing the experiment and interference noise is neglected. Moreover, binding noise refers to not-having/wrong binding events between virus and their antibodies.

The received concentration of pathogens can be expressed as [3]

$$C_r = \zeta\gamma C_{\text{mean}} + n \quad (6.7)$$

where ζ is the sampling (collection) efficiency for the aerosol sampler which is responsible for controlling the sampling rate of air and collecting the existing particles in air. Many technologies can be adapted for sampling. In [3], they consider an electrostatic precipitation-based sampler due to its sensitivity and ability in sampling nano-sized particles. Although pathogen-laden droplets are in the size of microme-

ters, pathogens are nanometer-sized. Moreover, an electrostatic aerosol sampler is commercially available and has an efficiency of 80%-90%. Furthermore, γ denotes the biding efficiency of the receiver, and $\hat{n}$ is additive noise resulting from flicker, thermal noise and other noise. It is modeled as Gaussian with zero mean and variance N_0^2. Here, we assume a cubic-shape receiver.

6.3 Deriving the Probability of Misdetection

In this section, we want to derive the probability of misdetection. We start by comparing C_{mean} with the maximum likelihood threshold C_{th} to decide whether the pathogens are detected at the receiver side $\mathcal{R}$ or not detected at the receiver side $\mathcal{N}$. Therefore, we use the decision rule

$$P(\mathcal{N}|C_r) \underset{\mathcal{R}}{\overset{\mathcal{N}}{\gtrless}} P(\mathcal{R}|C_r), \tag{6.8}$$

Using Bay's rule and given that the probability of detecting and not detecting pathogens at the receiver side are equally likely, we get

$$P(C_r|\mathcal{N}) \underset{\mathcal{R}}{\overset{\mathcal{N}}{\gtrless}} P(C_r|\mathcal{R}) \tag{6.9}$$

From (6.7), we write (6.9) as

$$\frac{1}{\sqrt{2\pi}N_0}\mathrm{e}^{\frac{-(C_r-\zeta\gamma C_{\text{mean}})^2}{2N_0^2}} \underset{\mathcal{R}}{\overset{\mathcal{N}}{\gtrless}} \frac{1}{\sqrt{2\pi}N_0}\mathrm{e}^{\frac{-(C_r)^2}{2N_0^2}} \tag{6.10}$$

We simplify the expression above,

$$C_r \underset{\mathcal{R}}{\overset{\mathcal{N}}{\gtrless}} \frac{\zeta\gamma C_{\text{mean}}}{2} \tag{6.11}$$

and thus

$$C_{\text{th}} = \frac{\zeta\gamma C_{\text{mean}}}{2} \tag{6.12}$$

Moreover, we write the probability of misdetection P_{md} as

$$P_{\text{md}} = (C_r \leq C_{\text{th}} | \mathcal{N}) \tag{6.13}$$

After doing some change of variables, we obtain

$$P_{\text{md}} = \mathbf{Q}\big(\frac{\zeta \gamma C_{\text{mean}}}{\sqrt{2^3 N_0}}\big) \tag{6.14}$$

where $\mathbf{Q}$ represent the $\mathbf{Q}$ function.

To find the probability of misdetection for the case of total reflection and partial absorption, we assume a point source as an approximation of the planar surface and then integrate over the receiver volume to find C_{mean}. In the figure below, we plot the P_{md} versus y_r where y_r indicates the receiver location along the $y-$direction and we choose the molecules source to be at $(0.6, 1.2, 1.7)$

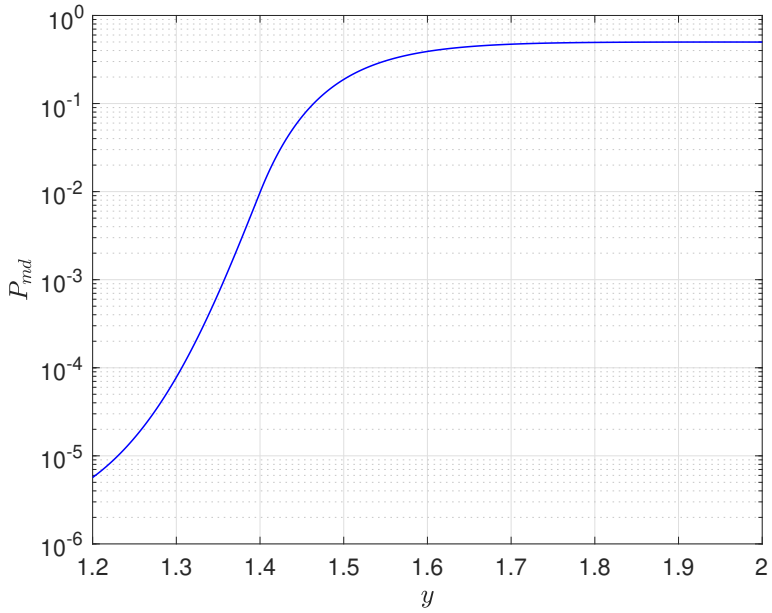

Figure 6.2: Impact of distance on P_{md}

In Fig. 6.2, we see that the probability of misdetection is small at $y = 1.2 - 1.4$

because the person is standing at $y = 1.2$. Then, P_{md} is increasing when the receiver is getting faraway from VOCs source till it reaches a constant value because the wall at $y = 2$ is a reflector.

Chapter 7

Conclusion and Future Work

In conclusion, we analyzed the communication through breath in a bounded indoor environment where we derive the mathematical model of the VOCs concentration. The walls of the environment could be reflective and/or absorptive. Moreover, we derive the probability of misdetection and find the concentration of molecules at the receiver and source. Also, we validate the performance of the mathematical models by showing some numerical results.

For future work, we can derive the concentration of VOCs where we have multiple transmitters and/or receivers. Furthermore, we can minimize the probability of misdetection by finding the best location for the transmitter and receiver.

REFERENCES

[1] T. Nakano, A. W. Eckford, and T. Haraguchi, *Molecular communication*. Cambridge University Press, 2013.

[2] N. Farsad, H. B. Yilmaz, A. Eckford, C.-B. Chae, and W. Guo, "A comprehensive survey of recent advancements in molecular communication," vol. 18, no. 3, pp. 1887–1919, 2016.

[3] M. Khalid, O. Amin, S. Ahmed, B. Shihada, and M.-S. Alouini, "Communication through breath: Aerosol transmission," vol. 57, no. 2, pp. 33–39, 2019.

[4] M. Khalid, O. Amin, S. Ahmed, B. Shihada, and M. Alouini, "Communication through breath: Aerosol transmission," *IEEE Communications Magazine*, vol. 57, no. 2, pp. 33–39, February 2019.

[5] B. J. Cowling, D. K. Ip, V. J. Fang, P. Suntarattiwong, S. J. Olsen, J. Levy, T. M. Uyeki, G. M. Leung, J. M. Peiris, T. Chotpitayasunondh *et al.*, "Aerosol transmission is an important mode of influenza A virus spread," *Nature Ccommun.*, vol. 4, p. 1935, 2013.

[6] A. Fernstrom and M. Goldblatt, "Aerobiology and its role in the transmission of infectious diseases," *J. Pathogens*, vol. 2013, 2013.

[7] S. O'Brien, "Getting the flu can wreak havoc on your finances," https://www.cnbc.com/2017/10/30/the-flu-costs-the-us-economy-10-point-4-billion.html, Oct. 2017.

[8] M. Khalid, O. Amin, S. Ahmed, and M.-S. Alouini, "System modeling of virus transmission and detection in molecular communication channels," in *IEEE Int. Conf. Commun. (ICC)*. IEEE, 2018, pp. 1–6.

[9] V. Jamali, A. Ahmadzadeh, W. Wicke, A. Noel, and R. Schober, "Channel modeling for diffusive molecular communication-a tutorial review," *arXiv preprint arXiv:1812.05492*, 2018.

[10] S. P. Arya *et al.*, *Air pollution meteorology and dispersion*. Oxford University Press New York, 1999, vol. 310.

[11] M. S. Gockenbach, *Partial Differential Equations: Analytical and Numerical Methods, Second Edition*, 2nd ed. Philadelphia, PA, USA: Society for Industrial and Applied Mathematics, 2010.

[12] J. W. Tang, A. D. Nicolle, C. A. Klettner, J. Pantelic, L. Wang, A. B. Suhaimi, A. Y. L. Tan, G. W. X. Ong, R. Su, C. Sekhar, D. D. W. Cheong, and K. W. Tham, "Airflow dynamics of human jets: Sneezing and breathing - potential sources of infectious aerosols," *PLOS ONE*, vol. 8, no. 4, pp. 1–7, 04 2013. [Online]. Available: https://doi.org/10.1371/journal.pone.0059970

APPENDICES

Appendix A

Proof of the Orthogonality of the Partial Absorption Basis

$$\frac{\partial^2 X}{\partial x} + \lambda^2 X = 0 \Longleftrightarrow \frac{d}{dx}\Big[\frac{dX}{dx}\Big] + \lambda^2 X = 0. \tag{A.1}$$

The boundary conditions are given as

$$\frac{\partial X(G_x)}{\partial x} - \beta_2 X(G_x) = 0, \tag{A.2}$$

$$\frac{\partial X(0)}{\partial x} - \beta_1 X(0) = 0. \tag{A.3}$$

$$[\phi_m']' + \lambda_m^2 \phi_m = 0, \tag{A.4}$$

$$[\phi_n']' + \lambda_n^2 \phi_n = 0. \tag{A.5}$$

Multiply (A.4) by ϕ_n and (A.5) by ϕ_m yields

$$[\phi_m']'\phi_n + \lambda_m^2 \phi_m \phi_n = 0, \tag{A.6}$$

$$[\phi_n']'\phi_m + \lambda_n^2 \phi_n \phi_m = 0. \tag{A.7}$$

Subtracting (A.6) from (A.7) gives the following

$$[\phi_n']'\phi_m - [\phi_m']'\phi_n + \lambda_n^2 \phi_n \phi_m - \lambda_m^2 \phi_m \phi_n = 0, \tag{A.8}$$

$$[\phi_n']'\phi_m - [\phi_m']'\phi_n + (\lambda_n^2 - \lambda_m^2)\phi_m\phi_n = 0. \tag{A.9}$$

Integrating both sides on the interval $[0, G_x]$ gives

$$\int_0^{G_x} \Big[[\phi_n']'\phi_m - [\phi_m']'\phi_n\Big]dx + \int_0^{G_x} (\lambda_n - \lambda_m)\phi_m\phi_n dx = 0. \tag{A.10}$$

To prove equation (A.10), we solve the two integrations

1) The first integration is solved using integration by part as follows

$$\int_0^{G_x} \Big[[\phi_n']'\phi_m - [\phi_m']'\phi_n\Big]dx = \int uv'dx = uv - \int u'vdx$$

$$= \phi_m\phi_n'\Big|_0^{G_x} - \int_0^{G_x} \phi_m'\phi_n' dx - \phi_n\phi_m'\Big|_0^{G_x} + \int_0^{G_x} \phi_n'\phi_m' dx \tag{A.11}$$

while $\int_0^{G_x} \phi_m'\phi_n' dx = \int_0^{G_x} \phi_n'\phi_m' dx = 0$

$$\int_0^{G_x} \Big[[\phi_n']'\phi_m - [\phi_m']'\phi_n\Big]dx = \phi_m\phi_n'\Big|_0^{G_x} - \phi_n\phi_m'\Big|_0^{G_x}$$

$$= \phi_m(G_x)\phi_n'(G_x) - \phi_m(0)\phi_n'(0) - \phi_n(G_x)\phi_m'(G_x) + \phi_n(0)\phi_m'(0). \tag{A.12}$$

Consider the boundary conditions in (A.2) and (A.3) as follows

$$\phi'(G_x) - \beta_2\phi(G_x) = 0 \quad \Rightarrow \quad \phi'(G_x) = \beta_2\phi(G_x), \tag{A.13}$$

$$\phi'(0) - \beta_1\phi(0) = 0 \quad \Rightarrow \quad \phi'(0) = \beta_1\phi(0). \tag{A.14}$$

Substitute the boundary conditions (A.13) and (A.14) in (A.12) yields

$$\phi_m(G_x)\phi_n'(G_x) - \phi_n(G_x)\phi_m'(G_x) = \beta_2\phi_m(G_x)\phi_n'(G_x) - \beta_2\phi_n(G_x)\phi_m'(G_x) = 0 \tag{A.15}$$

$$-\phi_m(0)\phi_n'(0) + \phi_n(0)\phi_m'(0) = -\beta_2\phi_m(0)\phi_n'(0) - \beta_2\phi_n(0)\phi_m'(0) = 0 \tag{A.16}$$

2)

$$\int_0^{G_x} (\lambda_n - \lambda_m)\phi_m\phi_n dx = 0 \qquad \text{if} \quad (\lambda_n - \lambda_m) \neq 0 \tag{A.17}$$

Therefore, (A.10) holds which results in having orthogonal basis since $\phi_m\phi_n = 0$.